



Published in final edited form as:

*Arthritis Rheum.* 2012 March ; 64(3): 762–771. doi:10.1002/art.33404.

## IFN $\gamma$ regulates discordant mechanisms of uveitis versus joint and axial disease in a murine model resembling spondyloarthritis

Jelena M Kezic, PhD<sup>1</sup>, Michael P Davey, MD, PhD<sup>2,3,5</sup>, Tibor T Glant, MD, PhD<sup>4</sup>, James T Rosenbaum, MD<sup>1,3</sup>, and Holly L Rosenzweig, PhD<sup>1,2,5</sup>

<sup>1</sup>Casey Eye Institute, Oregon Health & Science University, Portland, OR, USA

<sup>2</sup>Veterans Affairs Medical Center, Portland, OR, USA

<sup>3</sup>Department of Medicine, Oregon Health & Science University, Portland, OR, USA

<sup>4</sup>Departments of Biochemistry and Orthopedics, Rush University Medical Center, Chicago, IL, USA

<sup>5</sup>Department of Molecular Microbiology and Immunology, Oregon Health & Science University, Portland, OR, USA

### Abstract

**OBJECTIVE**—The spondyloarthropathies (such as ankylosing spondylitis) are multi-system inflammatory diseases that frequently result in uveitis, or intra-ocular eye inflammation. Despite the common co-occurrence of uveitis with arthritis, there has been no explanation for the eye's susceptibility to inflammation. Using an innovative intravital videomicroscopic approach, we discovered the co-existence of uveitis with axial and peripheral joint inflammation in mice immunized with cartilage proteoglycan (PG). Here, we elucidate the characteristics of uveitis and test the impact of IFN $\gamma$  deficiency on the eye versus the joint and spine.

**METHODS**—Female, TCR-Tg or IFN $\gamma$  knock-out crossed to TCR-Tg mice were immunized with PG. Uveitis was assessed by intravital videomicroscopy and histology. The clinical and histopathologic severity of arthritis and spondylitis were evaluated. Bone remodeling process within the spine was assessed by whole-body NIR imaging. Immunoblotting and immunofluorescence staining were used to examine expression of PG and ADAMTS-5 along with examination of the cellular composition of uveitic eyes.

**RESULTS**—PG neo-epitopes along with the aggrecanase, ADAMTS-5, are present in the eye as they are the joint. Anterior uveitis develops in response to PG immunization. The cellular infiltrate consists mainly of neutrophils and eosinophils. Unexpectedly, IFN $\gamma$  deficiency markedly exacerbates uveitis while ameliorating joint and spine disease, indicating divergent mechanisms that drive diseases in the eye versus joints and spine.

**CONCLUSIONS**—This is the first detailed description of a murine disease model wherein uveitis coincides with arthritis and spondylitis. Our observations provide great opportunity to understand the pathogenesis of a relatively common but poorly understood disease.

Many immune-mediated inflammatory diseases including systemic lupus erythematosus (SLE), rheumatoid arthritis, Sjogren's syndrome, Wegener's granulomatosis,

---

Please address correspondence to: Holly L. Rosenzweig, PhD, Oregon Health & Science University, Mail stop: L 467 AD, 3181 SW Sam Jackson Park Rd., Portland, OR 97239, Phone: 503-494-8157, Fax: 503-494-6875, rosenzwh@ohsu.edu.

Potential conflict of interest: J.T.R has been a consultant to Novartis and Amgen.

dermatomyositis, ankylosing spondylitis, inflammatory bowel disease, and psoriatic arthritis are multi-system diseases wherein multiple organs are afflicted but often divergently. This phenomenon has presented considerable challenges clinically in the treatment of patients suffering from multi-system inflammatory diseases. Experimentally, most animal models focus predominantly on a single organ. Very few animal models have attempted to clarify why 2 organ systems may develop discordant inflammatory activity. Uveitis, or intra-ocular inflammatory disease, is the most common, clinically important extra-articular manifestation of several inflammatory diseases including Behcet's disease, ankylosing spondylitis, juvenile idiopathic arthritis, and Blau syndrome. In fact, uveitis is associated with arthritis in at least 15 distinct clinical entities. Yet, despite the frequent co-existence of uveitis with multi-system diseases involving the joints, the underlying mechanisms that predispose to eye inflammation are poorly understood.

Uveitis is a leading cause of blindness and is comparable to diabetes or macular degeneration in terms of years of visual loss because it affects children as well as young adults (1). Ankylosing spondylitis (AS) and its closely related spondyloarthropathies, which are inflammatory diseases that involve the spine and sacroiliac joints in a characteristic pattern, are the most commonly diagnosed systemic diseases with uveitis in North America and Europe. As many as 50% of the patients with AS develop uveitis during their lifetime (2). The AS-associated uveitis is typically anterior, meaning it most consistently affects the iris, and typically manifests as unilateral with recurrent episodes (3). HLA-B27 is a documented genetic susceptibility factor for AS (4), and ~95% of patients with AS who develop uveitis are HLA-B27 positive (5); yet its presence only accounts for ~20–40% of the genetic risk for AS. Genetic studies and clinical observations strongly suggest that uveitis is affected by additional genetic or environmental factors that distinguish it from either axial or peripheral joint disease characteristic of AS (4, 6).

The major proteoglycan, aggrecan, (hereon referred to as PG) has been a reported autoantigen in AS (7). Experimental autoimmunity to PG results in progressive and chronic, erosive polyarthritis and axial spondylitis in genetically susceptible mice representative of the clinical spectrum of disease observed in patients with AS and related spondyloarthropathies (8, 9). Aggrecan consists of three globular domains (G1–G3) separated by interglobular domains (IGD). Epitope mapping studies have identified the dominant and most arthritogenic T cell epitopes (both in humans and mice) to be located in the G1 domain (10). Immunization with G1 domain sufficiently induces disease as does PG (11) and T cell receptor transgenic mice specific for the dominant arthritic epitope of the G1 domain of aggrecan ( $V\alpha 1.1$ ,  $V\beta 4$ ; denoted as TCR-Tg mice), develop an accelerated and more severe polyarthritis (12). In the proceedings of a recent meeting, we described a previously unreported uveitis coincident with arthritis and spondylitis in mice immunized with PG (13).

Here, using intravital videomicroscopy, a technique that allows us to visualize on-going inflammatory responses *in vivo* within the iris vasculature and tissue, we elucidated the onset and severity of uveitis as it progresses in relation to peripheral joint and axial inflammation in mice immunized with PG. We further investigated the function of the prototypical Th1-related cytokine, IFN $\gamma$ , in the pathogenesis of uveitis versus its role in peripheral arthritis or spondylitis. Somewhat surprisingly, we discover that IFN $\gamma$  plays divergent roles in disease of the eye versus joints and spine. Thus, the PG-immunization model of uveitis could provide insights into the mechanism of uveitis in the spondyloarthropathies.

## MATERIALS AND METHODS

### Mice

Transgenic mice over-expressing the T cell receptor (TCR) specific for the dominant arthritic epitope of the G1 domain of aggrecan (V $\alpha$ 1.1, V $\beta$ 4; referred to as TCR-Tg mice) backcrossed 10 generations onto BALB/c strain (12), along with TCR-Tg mice crossed with IFN $\gamma$ knock-out (KO) mice on BALB/c background (which were previously backcrossed 10 generations onto the BALB/c strain). (referred to as GKO/TCR-Tg mice) were housed in a facility approved by the Association of Assessment and Accreditation of Laboratory Animal Care International. Procedures followed National Institute of Health guidelines and Oregon Health & Science University Institutional Animal Care and Use policies.

### Purification of aggrecan (PG)

Cartilage PG was purified from human knee articular cartilage obtained from patients undergoing elective joint replacement surgery as previously described (10, 14). Briefly, cartilage pieces were pulverized under liquid nitrogen and extracted with guanidinium chloride in the presence of protease inhibitors and further purified by centrifugation and dialysis. The glycosaminoglycan side chains of PG were then digested with endo- $\beta$ -galactosidase (Seikagaku, Japan) and testicular hyaluronidase (Sigma, St. Louis, MO) in the presence of protease inhibitors, and further purified by centrifugation and dialysis. Samples were irradiated at 20,000 rads and stored at  $-80^{\circ}\text{C}$ .

### PG-immunization

For immunization, female, mice (16 weeks of age) were administered an intraperitoneal (i.p.) injection of 100  $\mu\text{g}$  of PG emulsified with 1.5 mg adjuvant dimethyl-dioctadecyl ammonium bromide (DDA; Sigma/Aldrich) in PBS along with 1.5  $\mu\text{g}$  of pertussis toxin (Sigma). Mice received an additional i.p. injection of pertussis toxin 48 hours later. Booster immunizations were administered the same way 3 weeks later. Adjuvant control animals received DDA and pertussis toxin alone. Mice were assessed weekly for clinical manifestations of peripheral arthritis in a masked fashion using an established scoring method as previously described (10, 14). The score ranged from 0 to 4 per paw based on swelling, redness, deformities and ankylosis. The data are represented as the cumulative score for all 4 paws, resulting in a maximum of 16 per mouse.

### Intravital microscopy

The leukocytic response within the vasculature and extravascular tissue of the iris was quantified by intravital video-microscopy according to previously established methodology (15, 16). Briefly, at the time of imaging animals were injected intraperitoneally with 35 mg/kg of rhodamine 6G (Sigma, St. Louis, MO, USA) and anesthetized with 1.7 % isoflurane. Digital images of 3 independent regions of the iris vasculature/tissue were captured with a black and white video camera (Kappa Scientific, Gleichen, Germany) on an epifluorescence intravital microscope (modified Orthoplan; Leica, Wetzlar, Germany) within 3 independent regions. Diameter and length of each vessel segment or iris tissue as well as leukocyte phenotype (i.e., rolling, adhering, infiltrating) were quantified off-line with Image J analysis software.

### Histopathology

All tissues (eyes, knees or spines) were fixed in 10% neutral-buffered formalin. Spine and joints were decalcified prior to paraffin embedding, and sectioned longitudinally (7  $\mu\text{m}$ ). Eyes were sectioned at 7  $\mu\text{m}$  through the pupillary-optic nerve axis at four different depths. Tissue sections were stained with hematoxylin and eosin (H&E). In the case of eye

histopathology, three sections from different levels of each eye were examined by a masked observer using a modified version of an ocular histopathology grading system (17), which rates inflammation based on cellular infiltration of the anterior and posterior eye segments, and structural/morphological changes to the retina.

### Immunoblotting

Protein was extracted from eye tissue in the presence of protease inhibitors, quantified and immunoblotting was performed as described previously (18). Expression of G1-neoepitope of aggrecan and ADAMTS5 were assessed using rabbit polyclonal anti-aggrecan (ABR-Affinity Bioreagents) and rabbit polyclonal anti-ADAMTS-5 (Abcam), respectively and detected with near-infrared (NIR)-fluorescently labeled secondary antibody (goat anti-rabbit IRDye-698, Licor-Odyssey).

### Immunofluorescence staining

Sections were de-paraffinized and rehydrated before antigen retrieval using 20 mM EDTA tetrasodium (Invitrogen). Sections were blocked for 60 min at room temperature (RT) using 5% bovine serum albumin (Sigma) containing 0.2% triton X-100 (Sigma). For aggrecan staining, sections were washed in chondroitinase buffer (0.1 Tris/acetate buffer, Ph 7.4) for 5 minutes before 45 min incubation in chondroitinase-ABC (Sigma) at 37°C. The following primary antibodies were applied to sections overnight at 4°C: rat anti-NIMP (R14, Abcam), anti-CCR3 (Y3L; Abcam), anti-CD3 (RM0027-3B19; Abcam), anti-CD45R/B220 (BD Pharmingen), anti-GFAP (DAKO), rabbit anti-mouse aggrecan (anti-aggrecan “G1-neoepitope [NITEGE<sup>373</sup>] (ABR Affinity Bioreagents), rabbit polyclonal IgG (Abcam), and isotype control rat, IgG2a or IgG2b (eBioscience). The secondary antibodies, Alexa Fluor-568 or Alexa Fluor-488 (Molecular Probes/Invitrogen), were applied for 2 hrs at RT, followed by DAPI (Roche) for 10 minutes. Sections were examined by confocal microscopy (Olympus Fluoview FV1000) and images spanning the full thickness of the tissue were produced by performing Z-stacks from the internal to external aspect at 1 µm increments. Adobe Photoshop (Version 7.0) was used for final image processing.

### In vivo Near-infrared (NIR) fluorescent imaging

Mice were administered an intravenous injection of 150 µl OsteoSense 680 (2nmol, ViseEn Medical), which is a NIR-fluorescent diphosphonate imaging agent that is incorporated into areas of microcalcifications and bone remodeling, thereby allowing us to specifically visualize on-going bone growth and resorption *in vivo*. NIR-fluorescence whole-body scanning was performed 24 h post-OsteoSense injection at the time of sacrifice using a Licor-Odyssey infrared imaging system with a MousePod attachment. Images were analyzed using commercially available software (Licor-Odyssey) for regions of interest over the spine and the mean differences in fluorescent intensity were quantified.

### Statistical analysis

All data are represented as mean ± SEM. Mean differences were compared and statistical differences were determined using analysis of two-way and one-way analysis of variance (ANOVA) with two-tailed, Students t-test post hoc analyses. In the case of comparisons of clinical arthritis scores or ocular histopathology scoring (i.e. nonparametric data), the Mann-Whitney U test was used (Prism; Graph Pad Software).

## RESULTS

### **The arthritogenic G1 domain of aggrecan along with the aggrecanase, ADAMTS-5, is expressed in murine and human ocular tissue**

Expression of the G1 domain of cartilage PG, which contains the arthritogenic T-cell epitopes, was examined in eye tissues. We find the presence of the G1-neoepitope within most murine and human ocular tissues (Figure 1A), and it is localized within the stroma of the iris tissue along with the nerve fiber layer of the retina (Figure 1B). We further show that ADAMTS-5 (aggrecanase-2), which is considered one of the major enzymes responsible for cleavage of PG and generation of G1- neoepitope(s) of PG in articular cartilage (19, 20) is also present in murine eye tissue (Figure 1C). These are one of the first demonstrations of an extra-articular presence of either the G1-neoepitope of PG or the aggrecanase, ADAMTS-5, within the eye tissues (21).

### **Experimental autoimmunity to PG results in uveitis and IFN $\gamma$ is an essential mediator of protection against uveitis**

Using intravital videomicroscopy (16), we evaluated the course of PG-induced intra-ocular inflammation within the iris vasculature and tissue, which is the most consistently affected tissue in anterior uveitis, using transgenic mice over-expressing the T cell receptor (TCR) specific for the dominant arthritic epitope of the G1 domain of PG (referred to as TCR-Tg mice) (12). We also tested the influence of the prototypical Th1-related cytokine, IFN $\gamma$ , on the onset and severity of uveitis as it relates to the induction of peripheral arthritis or spondylitis using IFN $\gamma$  knock-out (KO) mice crossed with TCR-Tg mice (herein abbreviated GKO/TCR-Tg). TCR-Tg mice immunized with PG demonstrate ongoing leukocyte rolling and adherence within the microvasculature of the iris along with extravasation of cells from the vessels into the iris tissue itself as depicted in still images captured by intravital microscopy (Figure 2B). In contrast, adjuvant controls show very minimal ocular inflammation. Quantification of leukocytic responses within the iris across time reveals a constitutive and progressive increase in the number of rolling, adhering and infiltrating leukocytes within the iris of TCR-Tg mice (Figure 2A). We find that these cellular responses are markedly exacerbated in TCR-Tg mice lacking IFN $\gamma$ . Of note, a transient remission in uveitis in GKO/TCR-Tg mice was observed at 4–5 weeks post immunization with inflammation returning by 6 weeks post immunization. The altered kinetics is akin to the clinical manifestations of uveitis in patients with AS or Behcet's disease, wherein uveitis presents as recurrent episodes.

Histopathological examination at 3 weeks following immunization reveals a mild anterior uveitis in TCR-Tg mice (Figure 2C) and cells that have infiltrated from the iris tissue into the aqueous of the anterior chamber and are noted near the ciliary body. Very little posterior involvement was observed in TCR-Tg mice, albeit occasional leukocytes were noted within the vitreous (arrow) that was accompanied by retinal vasculitis (arrow). In contrast, immunized GKO/TCR-Tg mice develop a florid inflammation of both the anterior and posterior eye segments with marked leukocytic presence within the vitreous, iris, ciliary body and choroid. IFN $\gamma$  deficiency also results in exacerbated retinal vasculitis, retinal folding and photoreceptor damage. Given the marked exacerbation of cellular inflammation in the absence of IFN $\gamma$ , counting individual cells in the vitreous proved difficult. We adopted a histopathology scoring system (using disease criteria such as numbers of cells, structural changes within the retina, and vasculitis) to quantify pathological changes, which demonstrated the significant protective role for IFN $\gamma$ . We noted that the uveitis was typically unilateral with ~70% incidence. However, the exacerbated uveitis in GKO/TCR-Tg mice coincides with increased incidence of uveitis as well as severity, except at week 5. We

observed recurrent pathology and increased histopathology scores at week 6 post immunization, which was worsened in the absence of IFN $\gamma$  (data not shown).

### Elucidation of the cellular composition in uveitic eyes

Using immunofluorescence staining, we evaluated the inflammatory cellular composition of uveitic eyes at 3 weeks post immunization (Figure 3). We find that neutrophils and eosinophils are the predominant cell type in both the anterior and posterior segments, which are further increased as a consequence of IFN $\gamma$ -deficiency. Although PG-arthritis is considered a T cell-dependent and autoantibody-mediated disease, the number of T cells actually entering the joint is quite small (22, 23). Our findings are similar in that we detect very few T or B cells within uveitic eyes at this time point. MHC-II expression is increased within the retina, and its expression coincides with activated or proliferating astrocytes, based on increased GFAP expression which is a marker of gliosis or activated Muller cells (Figure 3C). Similar cellular changes were observed at 6 weeks following immunization (data not shown).

### IFN $\gamma$ -deficiency attenuates PG-induced peripheral joint arthritis

That IFN $\gamma$  protects against uveitis may be somewhat surprising considering its previously established pathogenic role in PG-arthritis in WT-BALB/c mice with normal T cell repertoires (24). Here, we confirm its role in promoting arthritis in the TCR-Tg mouse line within the first 4 weeks as both the clinical scores (Figure 4A) and histological assessment (Figure 4B) demonstrated a reduction in arthritis in the GKO/TCR-Tg mice compared to mice with intact IFN $\gamma$  at 3 weeks. We noted that the protective effects of IFN $\gamma$ -deficiency in arthritis of the knee were not sustained such that by 6 weeks following PG-immunization arthritis was comparable to TCR-Tg mice with intact IFN $\gamma$ .

### Evaluation of a role for IFN $\gamma$ in PG-induced axial disease

Progression of spondylitis is a key feature of PG-immunity in WT-BALB/c mice (25), yet the influence of IFN $\gamma$  on axial disease is unknown. Histological examination of the spondylitis in TCR-Tg mice shows that despite minimal pathological changes at 3 weeks (Figure 5A), almost complete destruction of the intervertebral discs has occurred by week 6. This is in contrast to immunized GKO/TCR-Tg mice wherein the destruction to intervertebral discs and vertebral body fusion is markedly reduced. NIR-fluorescence whole-body imaging (Figure 5B), that in this case detects signal from OsteoSense 680, which is a NIR-fluorescent diphosphonate imaging agent incorporated into areas of microcalcifications and bone remodeling, allows us to visualize the progression of spondylitis *in vivo*. Using NIR-imaging as a secondary means of assessing the role of IFN $\gamma$  in the severity of spondylitis, we observe most significant increase in NIR-signal at 6 weeks post PG-immunization in the TCR-Tg mice; however the NIR-intensity is significantly diminished in mice lacking IFN $\gamma$ . Thus, in contrast to the eye, IFN $\gamma$  promotes both peripheral joint and axial disease.

## DISCUSSION

Although uveitis consistently occurs in multi-system diseases involving the joints, the underlying mechanisms that predispose to eye inflammation are poorly understood. Here, we find that PG neo-epitopes along with the aggrecanase, ADAMTS-5 are present in the eye as they are the joint; and that following immunization with PG, immune responses causing arthritis and spondylitis have the potential to enter the eye and trigger uveitis. Thus, uveitis is a previously unreported but major aspect of this model. Our current report shows surprisingly divergent inflammatory mechanisms with regards to the role of IFN $\gamma$  in the eye versus joint and axial disease. Although uveitis is a heterogeneous collection of diseases, there is a dearth of mouse models of anterior segment inflammation (15, 26–30). None of



these models bears much resemblance to the most common clinical form of uveitis, since neither arthritis nor spondylitis is characteristic of these model systems. Our observations could provide insight into underlying mechanisms of uveitis in multi-system disease.

The reason for the co-existence of uveal and joint inflammation is unexplained, although some compounds such as hyaluronic acid, type II collagen, and aggrecan are common to both organs. Our demonstration that G1 neo-epitopes of aggrecan as well as ADAMTS-5 are present within eye tissues suggests that the generation of immunogenic PG within the eye may be especially relevant to the pathogenesis of uveitis as it is to arthritis and disc inflammation. One hypothesis would be that T cell immunity to articular cartilage component(s) such as PG could initiate uveitis as occurs in arthritis. Somewhat surprisingly but not entirely unexpected is our observation that few infiltrated T cells were present in uveitic eyes. This would be analogous to the joint, wherein the number of T cells entering the joint is actually quite small (23). It may be that T cells play an important role for initiation of disease but that sustained tissue damage is mediated by the increased presence of granulocytes. Notably, the neutrophil and eosinophil predominance in uveitic eyes from mice lacking IFN $\gamma$  is similar to the observations in experimental autoimmune uveitis (EAU) (31), which is a T cell-dependent model. Future studies to address the presence and functional contribution of T cells will prove informative to uveitis.

Our observations regarding divergent effects of IFN $\gamma$  in the uveitis versus arthritis or spondylitis would not be unlike what has been observed clinically with the challenges of treating multi-system inflammatory diseases including rheumatoid arthritis, Crohn's disease, Behcet's disease, and AS. For example, the anti-TNF- $\alpha$ , etanercept, is effective in treating the arthritis symptoms in patients with AS but does not always improve uveitis in the same patients (32). In fact, there are some reports of patients actually developing uveitis while receiving TNF- $\alpha$  inhibitors (33), supporting the possibility that divergent mechanisms may exist between uveitis and arthritis. In each of these illnesses, the clinical response in one organ does not guarantee a clinical response in another organ or system. So while the multi-system nature of an illness indicates that different organs share similar pathogenetic mechanisms, the discordance in the clinical response indicates that it is critical to understand the unique aspects of inflammation in each organ system. Interestingly, genetic segregation of susceptibility to PG-induced arthritis versus PG-induced spondylitis (34) indicates that unique mechanisms are involved in the pathogenesis of the spondylitis compared to arthritis as well.

Induction of PG-induced arthritis is considered to be primarily a Th1 dependent disease and not an IL-17 disease (24, 35, 36); albeit in the absence of IFN $\gamma$  it appears that IL-17 does mediate arthritis (37) suggesting a combinatorial role. The prior studies were performed in WT-BALB/c mice with a normal T cell repertoire, and our studies here corroborate the pathogenic role of IFN $\gamma$  in peripheral joint disease in TCR-Tg mice. We further expand our understanding of IFN $\gamma$  in the progression of axial disease wherein based on histology and NIR-imaging we find that IFN $\gamma$  potentiates the severity of spondylitis. In contrast to the skeletal aspects of this disease, our findings suggest that the uveitis is not primarily a Th1-dependent disease as IFN $\gamma$ -deficiency worsened uveitis. Given that the Th1 and Th17 subsets are reciprocally regulated, it seems plausible that Th17 responses ensue in the absence of IFN $\gamma$  which contribute to uveitis. Th17 cells have been reported to play a role in the animal model of posterior uveitis, experimental autoimmune uveitis (EAU) (38) and have been implicated in uveitis clinically (39). The production of IL-17 and IFN $\gamma$  by primed T cells has been also linked to gliosis or activation of astrocytes *in vitro* (40) which we observed to be increased in the absence of IFN $\gamma$ . Future studies to investigate the contribution of Th17 responses to uveitis will be informative.

The milieu of the aqueous is thought to influence the outcome of uveitis (41) and given the increased presence of immunosuppressive factors that contribute to its immune privileged state the eye may regulate immune responses in a tissue-specific manner. IFN $\gamma$  appears to be a key distinguishing factor between the eye and joints as IFN $\gamma$ -independent mechanism of uveitis ensue despite predominate systemic Th1 responses that promotes both arthritis and spondylitis. Resistance to the Th1-related responses may be an underlying protective mechanism within the eye. Aside from the eye, the local microenvironment within other tissues has been increasingly recognized for its importance in influencing the plasticity of Th17 cells (42, 43). For example, experimental induction of diabetes can be transferred by Th17 cells, yet can be completely abrogated by blockade of IFN $\gamma$  (43). Likewise synovial Th17 cells appear to convert to Th1/17 and Th1 cells in human inflammatory arthritis (44). The Th17/1 enrichment within inflamed uveitic eyes may be driven by an especially permissive environment that promotes plasticity of the Th17 cells (e.g. high TGF $\beta$  levels in the eye). It will be interesting to consider the extent to which Th1 versus Th17 cell phenotypes are impacted within uveitic eye tissue.

Our novel observation of simultaneous uveal and synovial inflammation in a mouse could yield invaluable information about contrasting mechanisms in different portions of the body and could have an important impact on how we approach therapy in uveitic patients with multi-system, inflammatory diseases like AS.

## Supplementary Material

Refer to Web version on PubMed Central for supplementary material.

## Acknowledgments

Financial support: This work was supported by NIH (NEI grants EY019020 (H.L.R.); EY019604 (J.T.R)). H.L.R. also receives support from the American College of Rheumatology Research and Education Foundation along with the Research to Prevent Blindness Foundation. We are grateful to the William and Mary Bauman Foundation, the Stan and Madelle Rosenfeld Family Trust and the William C. Kuzell Foundation for their financial support.

We thank C. Kintzley, K. Goodwin and K. Dahlhausen for their assistance in the quantification of intravital microscopic images and histological preparations. We thank E.E. Vance, J. Clowers, and A. Woods and for their technical assistance along with S.R. Planck for his critical discussions.

## References

1. Nussenblatt RB. The natural history of uveitis. *International Ophthalmology*. 1990; 14:303–308. [PubMed: 2249907]
2. Zeboulon N, Dougados M, Gossec L. Prevalence and characteristics of uveitis in the spondyloarthropathies: a systematic literature review. *Ann Rheum Dis*. 2008; 67(7):955–9. [PubMed: 17962239]
3. Rosenbaum JT. Characterization of uveitis associated with spondyloarthritis. *Journal of Rheumatology*. 1989; 16:792–796. [PubMed: 2778762]
4. Thomas GP, Brown MA. Genetics and genomics of ankylosing spondylitis. *Immunol Rev*. 2010; 233(1):162–80. [PubMed: 20192999]
5. Feltkamp TEW. HLA B27, acute anterior uveitis, and ankylosing spondylitis. *Advances in Inflammation Research*. 1985; 9:211–216.
6. Martin TM, Zhang G, Luo J, Jin L, Doyle TM, Rajska BM, et al. A locus on chromosome 9p predisposes to a specific disease manifestation, acute anterior uveitis, in ankylosing spondylitis, a genetically complex, multisystem, inflammatory disease. *Arthritis Rheum*. 2005; 52(1):269–274. [PubMed: 15641041]



7. Zou J, Appel H, Rudwaleit M, Thiel A, Sieper J. Analysis of the CD8+ T cell response to the G1 domain of aggrecan in ankylosing spondylitis. *Ann Rheum Dis*. 2005; 64(5):722–9. [PubMed: 15539415]
8. Glant TT, Cs-Szabo G, Nagase H, Jacobs JJ, Mikecz K. Progressive polyarthritis induced in BALB/c mice by aggrecan from normal and osteoarthritic human cartilage. *Arthritis Rheum*. 1998; 41(6):1007–18. [PubMed: 9627010]
9. Glant TT, Finnegan A, Mikecz K. Proteoglycan-induced arthritis: immune regulation, cellular mechanisms, and genetics. *Crit Rev Immunol*. 2003; 23(3):199–250. [PubMed: 14584879]
10. Glant TT, Mikecz K. Proteoglycan aggrecan-induced arthritis: a murine autoimmune model of rheumatoid arthritis. *Methods Mol Med*. 2004; 102:313–38. [PubMed: 15286393]
11. Glant TT, Radacs M, Nagyri G, Olasz K, Laszlo A, Boldizsar F, et al. Proteoglycan (PG)-induced arthritis (PGIA) and recombinant human PG-G1 domain-induced arthritis (GIA) in BALB/c mice resembling two subtypes of rheumatoid arthritis. *Arthritis and Rheumatism*. 2011 Epub ahead of print. 10.1002/art.30261
12. Berlo SE, Guichelaar T, Ten Brink CB, van Kooten PJ, Hauet-Broeren F, Ludanyi K, et al. Increased arthritis susceptibility in cartilage proteoglycan-specific T cell receptor-transgenic mice. *Arthritis Rheum*. 2006; 54(8):2423–33. [PubMed: 16869010]
13. Rosenzweig HL, Martin TM, Planck SR, Jann MM, Smith JR, Glant T, et al. Anterior uveitis accompanies joint disease in a murine model resembling ankylosing spondylitis. *Ophthalmic Res*. 2008; 40:189–92. [PubMed: 18421237]
14. Rosenzweig HL, Jann MM, Glant T, Martin TM, Planck SR, Van Eden W, et al. Activation of nucleotide oligomerization domain 2 exacerbates a murine model of proteoglycan-induced arthritis. *J Leukoc Biol*. 2009; 85(4):711–8. [PubMed: 19129483]
15. Rosenzweig HL, Martin TM, Jann MM, Planck SR, Davey MP, Kobayashi K, et al. NOD2, the gene responsible for familial granulomatous uveitis, is essential in a mouse model of muramyl dipeptide-induced uveitis. *Investigative Ophthalmology & Visual Science*. 2008; 49(4):1518–24. [PubMed: 18385071]
16. Becker MD, Nobiling R, Planck SR, Rosenbaum JT. Digital video-imaging of leukocyte migration in the iris: intravital microscopy in a physiological model during the onset of endotoxin-induced uveitis. *J Immunol Methods*. 2000; 240(1–2):23–37. [PubMed: 10854598]
17. Dick AD, Cheng YF, Liversidge J, Forrester JV. Immunomodulation of experimental autoimmune uveoretinitis: a model of tolerance induction with retinal antigens. *Eye*. 1994; 8(1):52–9. [PubMed: 8013720]
18. Rosenzweig H, Galster K, Planck S, Rosenbaum J. NOD1 expression in the eye and functional contribution to IL-1{beta} dependent ocular inflammation in mice. *Invest Ophthalmol Vis Sci*. 2009; 50(4):1746–53. [PubMed: 19074813]
19. Sandy JD, Verscharen C. Analysis of aggrecan in human knee cartilage and synovial fluid indicates that aggrecanase (ADAMTS) activity is responsible for the catabolic turnover and loss of whole aggrecan whereas other protease activity is required for C-terminal processing in vivo. *Biochem J*. 2001; 358(Pt 3):615–26. [PubMed: 11535123]
20. Struglics A, Larsson S, Pratta MA, Kumar S, Lark MW, Lohmander LS. Human osteoarthritis synovial fluid and joint cartilage contain both aggrecanase- and matrix metalloproteinase-generated aggrecan fragments. *Osteoarthritis Cartilage*. 2006; 14(2):101–13. [PubMed: 16188468]
21. Keller KE, Bradley JM, Acott TS. Differential effects of ADAMTS-1, -4, and -5 in the trabecular meshwork. *Investigative Ophthalmology & Visual Science*. 2009; 50(12):5769–77. [PubMed: 19553617]
22. Mikecz K, Glant T. Migration and homing of lymphocytes to lymphoid and synovial tissues in proteoglycan-induced murine arthritis. *Arthritis and Rheumatism*. 1994; 37(9):1395–403. [PubMed: 7945505]
23. Angyal A, Egleston C, Kobezda T, Olasz K, Laszlo A, Glant TT, et al. Development of proteoglycan-induced arthritis depends on T cell-supported autoantibody production, but does not involve significant influx of T cells into the joints. *Arthritis Res Ther*. 2010; 12(2):R44. Epub. [PubMed: 20298547]

24. Finnegan A, Mikecz K, Tao P, Glant TT. Proteoglycan (aggrecan)-induced arthritis in BALB/c mice is a Th1-type disease regulated by Th2 cytokines. *J Immunol.* 1999; 163(10):5383–90. [PubMed: 10553063]
25. Bardos T, Szabo Z, Czipri M, Vermes C, Tunyogi-Csapo M, Urban RM, et al. A longitudinal study on an autoimmune murine model of ankylosing spondylitis. *Ann Rheum Dis.* 2005; 64(7):981–7. [PubMed: 15640265]
26. Caspi RR, Grubbs BG, Chan C-C, Chader GJ, Wiggert B. Genetic control of susceptibility to experimental autoimmune uveoretinitis in the mouse model. *Journal of Immunology.* 1992; 148:2384–2389.
27. Bora NS, Kim MC, Kabeer NH, Simpson SC, Tandhasetti MT, Cirrito TP, et al. Experimental autoimmune anterior uveitis. *Investigative Ophthalmology & Visual Science.* 1995; 36:1056–1066. [PubMed: 7730015]
28. DeVoss J, Hou Y, Johannes K, Lu W, Liou GI, Rinn J, et al. Spontaneous autoimmunity prevented by thymic expression of a single self-antigen. *J Exp Med.* 2006; 203(12):2727–35. [PubMed: 17116738]
29. Dullforce PA, Seitz GW, Garman K, Michael JA, Crespo SM, Fleischman RJ, et al. Antigen specific accumulation of naive, memory and effector CD4T cells during anterior uveitis monitored by intravital microscopy. *Cell Immunol.* 2006; 239:49–60. [PubMed: 16712823]
30. Rosenbaum JT, McDevitt HO, Guss RB, Egbert PR. Endotoxin-induced uveitis in rats as a model for human disease. *Nature.* 1980; 286:611–613. [PubMed: 7402339]
31. Su SB, Grajewski RS, Luger D, Agarwal RK, Silver PB, Tang J, et al. Altered chemokine profile associated with exacerbated autoimmune pathology under conditions of genetic interferon-gamma deficiency. *Invest Ophthalmol Vis Sci.* 2007; 48(10):4616–25. [PubMed: 17898285]
32. Smith JR, Levinson RD, Holland GN, Jabs DA, Robinson MR, Whitcup SM, et al. Differential efficacy of tumor necrosis factor inhibition in the management of inflammatory eye disease and associated rheumatic disease. *Arthritis & Rheumatism.* 2001; 45(3):252–257. [PubMed: 11409666]
33. Lim LL, Fraunfelder FW, Rosenbaum JT. Do tumor necrosis factor inhibitors cause uveitis? A registry-based study. *Arthritis Rheum.* 2007; 56(10):3248–52. [PubMed: 17907169]
34. Szabo Z, Szanto S, Vegvari A, Szekanecz A, Mikecz K, Glant TT. Genetic control of experimental spondylarthropathy. *Arthritis and Rheumatism.* 2005; 52(8):2452–60. [PubMed: 16059927]
35. Cao Y, Doodes PD, Glant TT, Finnegan A. IL-27 induces a Th1 immune response and susceptibility to experimental arthritis. *J Immunol.* 2008; 180(2):922–30. [PubMed: 18178832]
36. Doodes PD, Cao Y, Hamel KM, Wang Y, Farkas B, Iwakura Y, et al. Development of Proteoglycan-Induced Arthritis Is Independent of IL-17. *J Immunol.* 2008; 181(1):329–37. [PubMed: 18566398]
37. Doodes PD, Cao Y, Hamel KM, Wang Y, Rodeghero RL, Mikecz K, et al. IFN-gamma regulates the requirement for IL-17 in proteoglycan-induced arthritis. *J Immunol.* 2010; 184(3):1552–9. [PubMed: 20028652]
38. Luger D, Silver PB, Tang J, Cua D, Chen Z, Iwakura Y, et al. Either a Th17 or a Th1 effector response can drive autoimmunity: conditions of disease induction affect dominant effector category. *J Exp Med.* 2008; 205(4):799–810. [PubMed: 18391061]
39. Amadi-Obi A, Yu CR, Liu X, Mahdi RM, Clarke GL, Nussenblatt RB, et al. TH17 cells contribute to uveitis and scleritis and are expanded by IL-2 and inhibited by IL-27/STAT1. *Nat Med.* 2007; 13(6):711–8. [PubMed: 17496900]
40. Jiang G, Ke Y, Sun D, Han G, Kaplan HJ, Shao H. Reactivation of uveitogenic T cells by retinal astrocytes derived from experimental autoimmune uveitis-prone B10RIII mice. *Invest Ophthalmol Vis Sci.* 2008; 49(1):282–9. [PubMed: 18172104]
41. Verma MJ, Lloyd A, Rager H, Strieter R, Kunkel S, Taub D, et al. Chemokines in acute anterior uveitis. *Current Eye Research.* 1997; 16:1202–1208. [PubMed: 9426952]
42. Lee YK, Turner H, Maynard CL, Oliver JR, Chen D, Elson CO, et al. Late developmental plasticity in the T helper 17 lineage. *Immunity.* 2009; 30(1):92–107. [PubMed: 19119024]

43. Bending D, De La Pena H, Veldhoen M, Phillips JM, Uyttenhove C, Stockinger B, et al. Highly purified Th17 cells from BDC2.5NOD mice convert into Th1-like cells in NOD/SCID recipient mice. *Journal of Clinical Investigation*. 2009; 119(3):565–572. [PubMed: 19188681]
44. Nistala K, Adams S, Cambrook H, Ursu S, Olivito B, de Jager W, et al. Th17 plasticity in human autoimmune arthritis is driven by the inflammatory environment. *PNAS*. 2010; 107(33):14751–14756. [PubMed: 20679229]

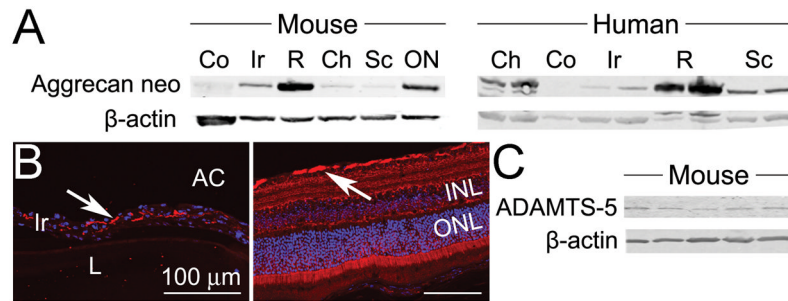


**Figure 1. Neo-epitope of G1 domain of aggrecan and ADAMTS-5 are expressed in ocular tissue**  
**Panel A)** Western blot analysis of eye tissues dissected from naive mice (left panel, pooled tissues from 10 individual mice) or human (representative blot of 2 individuals, right panel) probed with anti-G1-neoepitope (NITEGE<sup>373</sup> in the IGD) of aggrecan. The IGD between the G1 and G2 domains is the most sensitive region for MMP and aggrecanase cleavage, and the “G1-neoepitope” detected here (NITEGE<sup>373</sup>) represents the C-terminal end of ADAMTS-5-cleaved IGD retained in the tissue via the G1 domain bound to hyaluronan. **Panel B)** Eye sections from naïve mice were stained with anti-G1 neoepitope Ab (red) and DAPI (blue) for nuclear staining. Positive, red immunofluorescence signal (indicated by arrows) is observed within the iris stroma (left panel) and nerve fiber layer of the retina (right panel) (original magnification 200X). Staining with IgG isotype control antibody was negative (not shown). **Panel C)** Western blot of eye tissue homogenates from individual, naïve mice probed with anti-ADAMTS-5 Ab. Co = cornea; Ir = iris; R = retina; Ch = choroid; Sc = sclera; ON = optic nerve; INL = inner nuclear layer; ONL = outer nuclear of the retina.

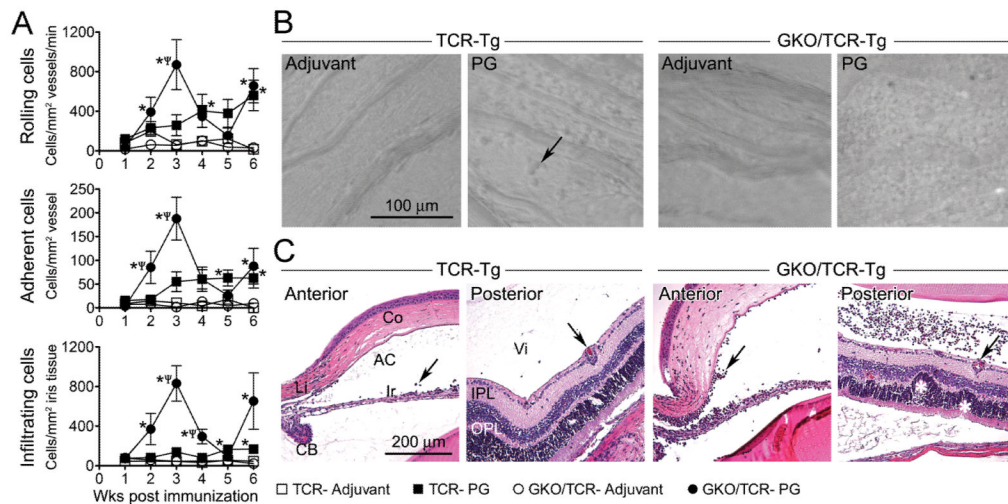


**Figure 2. Evaluation of IFN $\gamma$ -deficiency on the onset and severity of uveitis in response to PG immunization**

**Panel A)** Quantification of intravital videomicroscopy enumerating the number of rolling, adhering and infiltrating leukocytes as a function of time following immunization in TCR-Tg mice versus GKO/TCR-Tg mice. \*  $p < 0.05$  comparison for PG vs adjuvant within a genotype;  $\psi p < 0.05$  comparison for genotypic differences in PG-immunize mice ( $n = 9-12$  mice/treatment/genotype/time-point). **Panel B)** Representative still images of the microvasculature of the iris captured by intravital videomicroscopy at 3 weeks following immunization, arrow indicates an example of a leukocyte that has infiltrated the iris tissue. Note the marked increase in infiltrated leukocytes within iris tissue of the GKO/TCR-Tg mice (far right panel). **Panel C)** Representative histopathology images (original magnification 200X) of the anterior and posterior eye segments at 3 weeks following immunization. Infiltrated leukocytes and retinal vasculitis are indicated by arrows and retinal folding is marked by white asterisk.

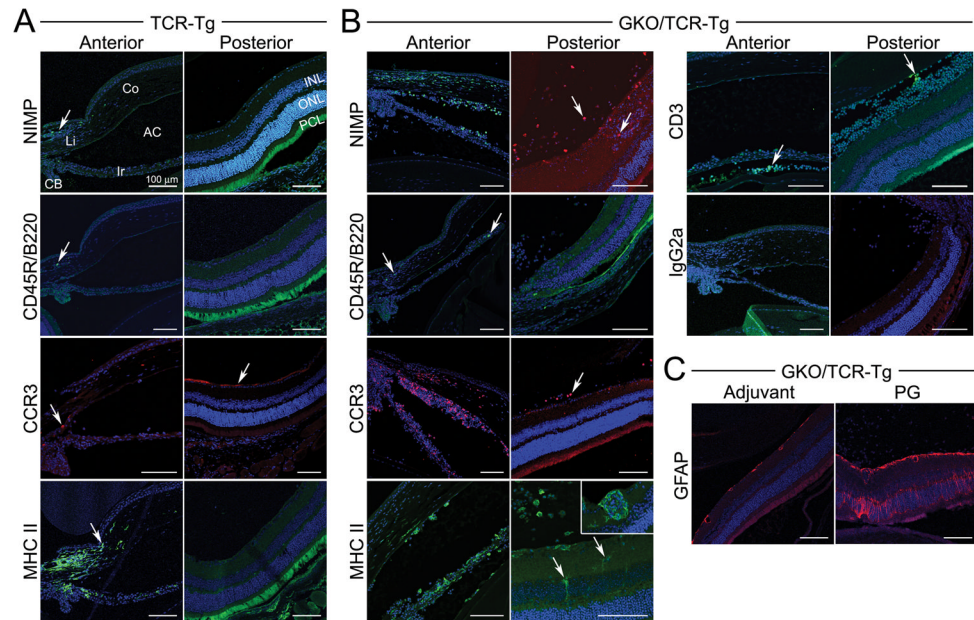


**Figure 3. Immunofluorescence staining of uveitic eyes at 3 weeks following immunization**  
 Eye sections of PG-immunized TCR-Tg (**panel A**) or GKO/TCR-Tg mice (**panel B**) that were stained with antibodies for the indicated cell markers (original magnification, 200X): NIMP = neutrophil, CD45R/B220 = B cell, CCR3 = eosinophil (red), MHC Class II (with inset of higher magnification, 400X), CD3 = T cell and IgG2a indicates negative staining in the control antibody group. **Panel C**) Staining for retinal glial fibrillary acid protein (GFAP) expression within the retina of GKO/TCR-Tg mice in adjuvant controls is increased after immunization, indicating gliosis or astrocyte activation/proliferation. Co = cornea; Ir = iris; CB = ciliary body; AC = anterior chamber; Vi = vitreous; INL, inner nuclear layer, ONL = outer nuclear layer; PCL, = photoreceptor cell layer.



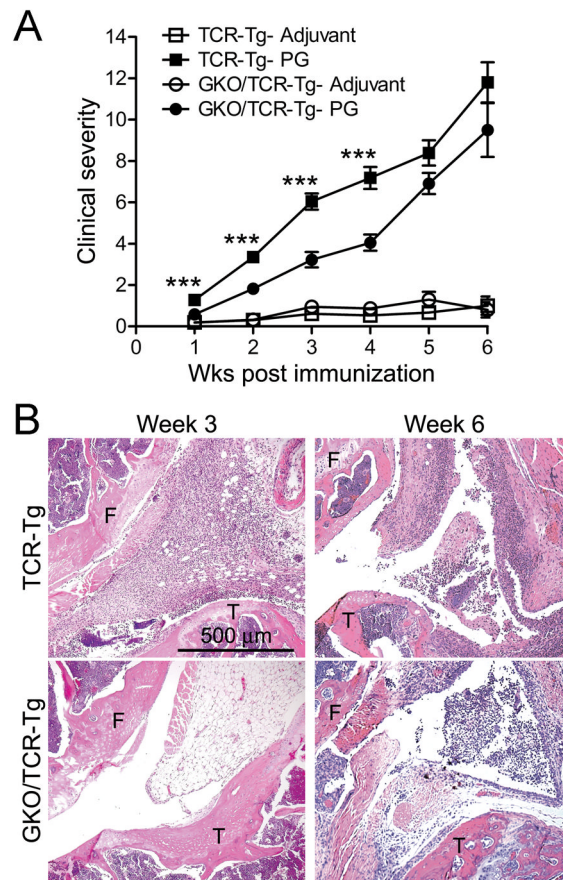


**Figure 4. IFN $\gamma$ -deficiency attenuates PG-induced peripheral joint arthritis**

**Panel A)** Clinical arthritic scores over course of disease. \*\*\*  $p < 0.001$  comparison between genotypes of PG-immunized mice ( $n = 9-12$  mice/treatment/genotype/time-point). **Panel B)** Representative histological images of arthritic knees (at 3 or 6 weeks post immunization (F = femur; T = tibia;))

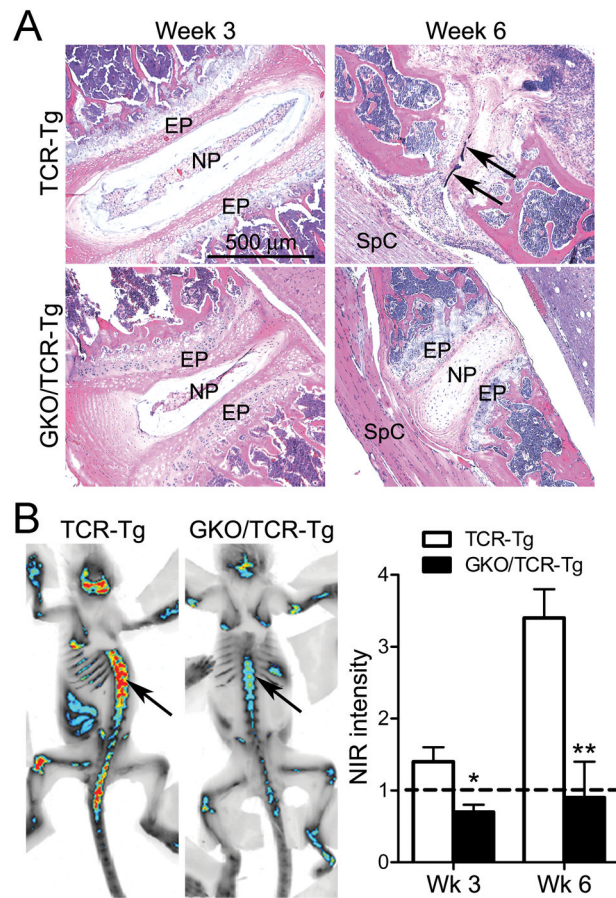


**Figure 5. IFN $\gamma$ -deficiency attenuates PG-induced spondylitis**

**Panel A)** Representative histological images of spine at 3 or 6 weeks post immunization (EN = endplate; NP = nucleus pulposus; SpC = spinal cord). **Panel B)** Representative images of NIR-fluorescence whole-body imaging at 6 weeks post immunization. Intensity of signal within the spine (arrow) indicates areas of microcalcification and bone remodeling (red = most intense signal and blue = less intense signal). Quantification (right panel) of the intensity of NIR-signal normalized to adjuvant-control mice (dashed line) was examined at 3 and 6 weeks post immunization; \* p < 0.05, \*\* p < 0.008 comparison between genotypes of PG-immunized mice (n = 6 mice/treatment/genotype/time-point).